LEGIBILITY NOTICE

A major purpose of the Technical Information Center is to provide the broadest dissemination possible of information contained in DOE's Research and Development Reports to business, industry, the academic community, and federal, state and local governments.

Although portions of this report are not reproducible, it is being made available in microfiche to facilitate the availability of those parts of the document which are legible.

3

LA-UR -90-1374

Los Alamos National Laboratory is operated by the University of California for the United States Department of Energy under contract W-7405-ENG-36

LA-UR--90-1374

DE90 010611

TITLE: Forced Convection Film Boiling Drag and Heat Transfer of a Wedge

AUTHOR(S) P. R. Chappidi
F. S. Gunnerson
K. O. Pasamehmetoglu

SUBMITTED TO AIAA/ASME Fifth Thermal Physcis and Heat Transfer Conference
June 18-20, 1990
Seattle, Washington

DISCLAIMER

Los Alamos Los Alamos National Laboratory
Los Alamos, New Mexico 87545

FORCED CONVECTION FILM BOILING DRAG AND HEAT TRANSFER OF A WEDGE

P.R. Chappidi,* F. S. Gunnerson** and K. O. Pasamehmetoglu+
Los Alamos National Laboratory
Nuclear Technology and Engineering Division
Engineering and Safety Analysis Group, Mail Stop K-557
Los Alamos, NM 87545

**University of Central Florida
Dept. of Mechanical Engineering
P.O. Box 25000
Orlando, FL 32816

Abstract

Laminar forced convection film boiling flow on a wedge is analyzed considering the streamwise pressure gradient imposed on the flow and the streamwise buoyancy force (important because of the large density difference between the vapor and liquid) acting on the vapor film. A two-phase boundary layer model is proposed, and the local similarity concept is applied to obtain an approximate solution of the governing equations. Parametric trends in this analysis show that, for a water-steam system at atmospheric pressure considered within this study, the density difference between the vapor and liquid is large enough. As a result, both the streamwise pressure gradient and the buoyancy force exert strong influence on the vapor flow dynamics. Wall skin friction results display a strong dependency on the streamwise buoyancy force driving the vapor film and the external pressure gradient. Previously observed "skin friction bucket" type phenomena with increased heating of the wedge are possible when the buoyancy force is small or negligible. Adverse streamwise buoyancy force acting on the vapor film, which is the case on the lower surface of a horizontally aligned wedge, may cause vapor flow separation. In contrast to wall skin friction dependency, the wall heat-transfer parameter shows a secondary dependence on the streamwise pressure gradient and the buoyancy force.

Nomenclature

C	Constant appearing in $U_e = C\, x^m$
C_{fx}	Local skin friction coefficient
C_p	Specific heat
f	Nondimensional stream function of liquid flow
Fr	Froude number $(U_e^2/U_o L_c g_x)$
g	Nondimensional stream function of vapor flow
h_x	Local heat-transfer coefficient
h_{fg}	Latent heat of vaporization
Ja_L	Jakob number of liquid $(C_{pL}(T_{sat} - T_\infty)/h_{fg})$
Ja_v	Jakob number of vapor $(C_{pv}(T_\infty - T_{sat})/h_{fg})$
k	Thermal conductivity of fluid
L_c	Characteristic length of the wedge
m	Pressure gradient parameter
$\dot{m}$	Mass flow rate of vapor per unit area
Nu_x	Local Nusselt number
P	Pressure
Pr	Prandtl number
q''_w	Local wall heat flux
R	Nondimensional density-viscosity product ratio $(\rho_v \mu_v / \rho_L \mu_L)$
Re_x	Local liquid Reynold's number $(\rho_L U_\infty x / \mu_L)$
$Re_{\delta v}$	Vapor film Reynold's number $(\rho_v u_I \delta_v / \mu_v)$
T	Temperature
T_{sat}	Saturation temperature
T_w	Wall temperature
T_∞	Free-stream liquid temperature
u	Stream-wise component of velocity
u_I	Interfacial (liquid-vapor interface) velocity
U_e	Liquid free-stream velocity
U_o	Reference velocity
v	Vertical component of velocity
x	Stream-wise coordinate
y	Normal coordinate
δ_v	Vapor film thickness
η	Nondimensional normal coordinate
$\eta_{v\delta}, \eta_{L\delta}$	Nondimensional vapor film thickness
λ	Nondimensional stream-wise coordinate, $2\xi(\rho_L - \rho_v)/Fr\rho_v$
ξ	Nondimensional stream-wise coordinate, $(x/L_c)^{m+1}/(m+1)$
β	Pressure gradient parameter, $2m/(m+1)$
μ	Absolute viscosity
ρ	Density
τ	Shear stress
Ψ	Stream function

Subscripts

v	Vapor
L	Liquid

Superscripts

'	Differentiation with respect to η_L or η_v as applicable

Introduction

In the recent past, several investigations[1-5] have been initiated to understand the influence of boiling on the drag of objects. Such information is of interest in analyzing external two-phase flow in many applications, including drag reduction[1,2] and molten fuel relocation in postulated nuclear reactor mishap scenarios.[4] In this connection, subcooled forced convection film boiling is analyzed for a wedge geometry. The choice of wedge geometry was motivated by the fact that a streamwise pressure gradient can be imposed on the flow, which is the case for a flow over any finite-thickness bodies such as a circular cylinder and sphere. Additionally, the results of the wedge flow serve as a guide in understanding film boiling flow and heat transfer on cylindrical and spherical geometries, and these results may be used to devise approximate solutions. In this paper, a comprehensive two-phase boundary layer model, unlike earlier models,[6-8] that takes the buoyancy force driving the vapor film and the stream-wise pressure gradient into account is proposed and analyzed.

Flow film boiling is analyzed by considering a subcooled liquid ($T_\infty < T_{sat}$) with a velocity U_e flowing towards an isothermal wedge as shown in Fig. 1. (Figure 1 shows a semi-infinite wedge in vertical and horizontal orientations, the orientation is important

---

* Post Doctoral Fellow, Member AIAA
** Associate Professor
\+ Staff Member

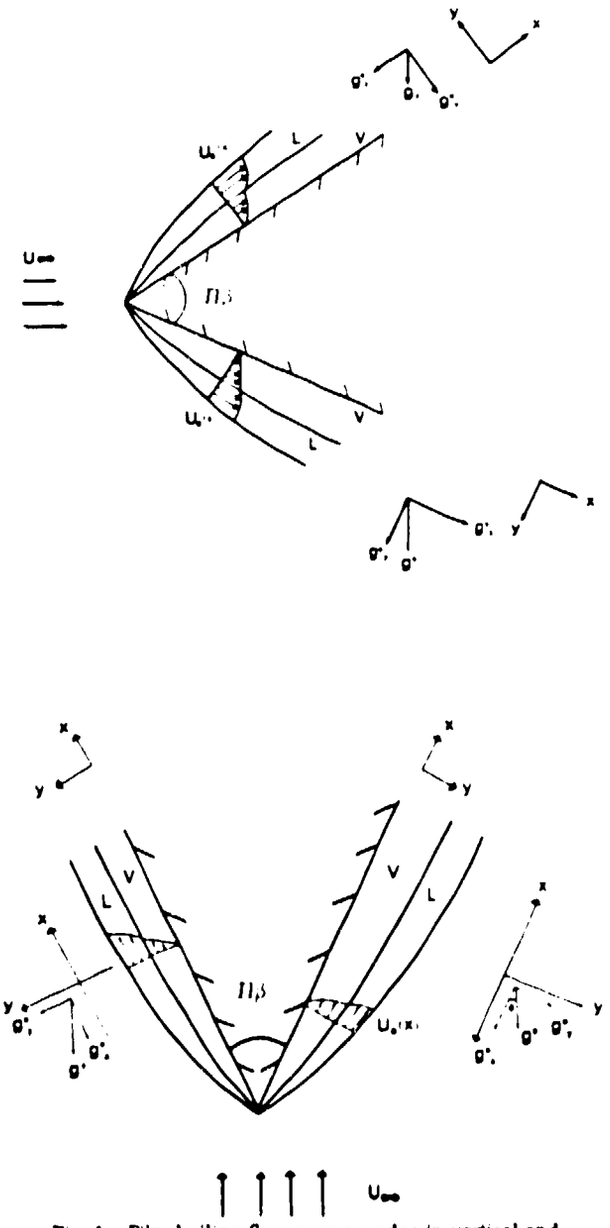

Fig. 1. Film boiling flow over a wedge in vertical and horizontal orientations.

with respect to the buoyancy effects on the flow as will be described later.) If the temperature of the wedge is assumed to be sufficiently high to promote and maintain stable film boiling conditions, a thin vapor film forms adjacent to the wedge surface. Subcooled liquid flows on top of this vapor film. Past analytical efforts, including the current one, describe the vapor film and liquid flow by boundary layer behavior. (The vapor film in forced convection film boiling is thin and amenable to the boundary layer approach, and the viscosity and temperature differential between the liquid free stream and the liquid-vapor interface leads to thermal and momentum boundary layer formation in the liquid flow.) This approach, called the two-phase boundary layer concept, originally was proposed by Cess and Sparrow.[2]

Walsh and Wilson[6] analyzed the film boiling flow on a wedge and obtained asymptotic expressions for two limiting cases corresponding to small and large subcoolings of liquid. They concluded that the stream-wise pressure gradient exerted on the vapor flow dominates the vapor flow dynamics and attributed this to the amplification of the pressure gradient effect on the vapor flow caused by the large density difference between the liquid and vapor. Nakayama's recent analysis[7] considered the same wedge flow geometry, neglecting inertial and convective terms in the vapor flow momentum and energy equations. He concludes that the local wall skin friction parameter exhibits a bucket-type behavior with increased heating of the wedge, when the liquid subcooling is small. Our subsequent effort[8] retained these terms and examined their significance; a simple couette flow model was proposed to explain some of the physics of the results. For a water-steam system at atmospheric pressure, the effect of including the convective energy terms within the vapor flow energy equation was found to be negligible, however, the inertial terms within the vapor flow momentum equation were found to exert considerable influence on the results at saturated liquid conditions.

None of the analyses[6-8] consider the influence of the stream-wise buoyancy force on flow film boiling. For example, at atmospheric pressure for a water-steam system, the density difference between the vapor and liquid is of the order of 1000, and the buoyancy force driving the vapor film over the wedge may be of the same order of magnitude as the other terms in the vapor flow momentum equation. This may exert an equally dominating effect on the vapor flow dynamics as the stream-wise pressure gradient. Unless the wedge is "very thin" and lies in horizontal orientation (implying that the stream-wise gravitational force component in the vapor flow momentum equation is negligible) or the Froude number is very large, the buoyancy force may have to be considered in the analysis. Consequently, the analyses[6-8] neglecting the effect of the buoyancy force may be valid only for horizontal wedges with a small included angle.[8] As to be demonstrated in this paper, several of the flow situations in forced convection film boiling may mandate the consideration of the buoyancy force on the vapor flow, which reveals several new features of flow physics.

This analysis, a continuation of our previous effort,[8] considers the influence of the stream-wise buoyancy force and the pressure gradient on the vapor flow. Because of this consideration, exact similarity conditions are not satisfied, complicating the analysis. By using a local similarity technique and a fourth-order Runge-Kutta method, a numerical solution is obtained for the governing equations. Parametric analysis for a water-steam system at atmospheric pressure is performed to understand the influence of boiling on skin friction drag and wall heat transfer.

The results of this analysis reveal that, unlike the horizontal flat plate geometry, the skin friction on a wedge in a film boiling flow may increase beyond the single-phase (all-liquid) flow level. This feature is attributed to the domination of the stream-wise buoyancy force and the stream-wise pressure gradient both driving the vapor flow. A turn-around behavior of the wall skin friction parameter with increased heating of the wedge (as demonstrated by earlier studies[6,8]) is possible only when the buoyancy force driving the vapor film is "low." On the lower surface of a horizontally aligned wedge in a film boiling flow, the buoyancy force on vapor film acts adversely to the flow direction. The current study demonstrates the possibility of flow separation under such conditions; a feature unnoticed until now. However, wall heat-transfer predictions, as opposed to skin friction predictions, do not demonstrate a strong dependency on the buoyancy force.

Analysis

Consider the physical model shown in Fig. 1, where the subcooled liquid ($T_\infty < T_{sat}$) with a velocity U_∞ flows towards an isothermal wedge. As discussed in the introduction, in a stable film boiling flow, a thin vapor film is assumed to form adjacent to the wedge surface and liquid flows on top of the vapor film. Several investigators have modeled the thin vapor film flow and the liquid flow assuming a boundary layer behavior.[1-3,5-8] Subsequently, the boundary layer equations of both liquid and vapor flow are coupled at the liquid-vapor interface by the appropriate conservation equations. This so called "two-phase boundary layer" concept used by all the previous investigators[1-3,5-8] (including the present analysis) incorporates the following assumptions, which are itemized briefly below

1. Steady, two-dimensional, incompressible and laminar flow is assumed in both phases.
2. Properties of both phases are estimated using the "film" temperature method.
3. Radiation from the solid surface is negligible.
4. The liquid-vapor interface is assumed to be smooth and at constant saturation temperature. Surface tension effects are neglected.
5. The liquid free-stream velocity is unaffected by the presence of the vapor and liquid boundary layers.

The incompressibility assumption is best justified at low velocities ($U_\infty < 15$ ft/s),[1] and the laminar flow assumption in the vapor film requires $Re_\delta \leq 100$.[9] For a water-steam system at atmospheric pressure such as the one considered in this model, property variations ($\rho_v, \mu_v, k_v, \mu_l$) may be included, and such treatment requires a variable fluid property analysis. Instead of such an approach, fluid properties are assumed constant, and the film temperature method, as suggested earlier,[10] is used to estimate the fluid properties. Radiation heat transfer from the surface may be neglected as the calculations (assuming black surface and using the experimental data of Stevens and Witte[11]) reveal that its contribution to forced convection film boiling heat transfer under atmospheric conditions for a subcooled water-steam system is less than 1%. Our recent analysis[12] shows that the theoretical wall heat-transfer predictions made neglecting radiation show little difference under subcooled flow conditions. The smooth liquid-vapor interface assumption, although difficult to realize in practice, has been reported at a high liquid subcooling.[1,11] Away from the leading edge where the boundary layer equations are applicable, the curvature of the liquid-vapor interface is less, and consequently the surface tension effects may be unimportant.

With the two-phase boundary layer concept that incorporates the above assumptions, governing equations can be derived for each phase and coupled at the liquid-vapor interface by the appropriate conservation equations.[3] The governing equations [Eqs. (1)–(16)] are summarized below.

VAPOR ($y < \delta_v$)

$$\frac{\partial u_v}{\partial x} + \frac{\partial v_v}{\partial y} = 0 \tag{1}$$

$$\rho_v \left(u_v \frac{\partial u_v}{\partial x} + v_v \frac{\partial u_v}{\partial y} \right) = - \frac{dp_v}{dx} + \mu_v \frac{\partial^2 u_v}{\partial y^2} + (\rho_l - \rho_v) g_x \tag{2}$$

$$\frac{\partial p_v}{\partial y} = 0 \tag{3}$$

$$\rho_v C_{pv} \left(u_v \frac{\partial T_v}{\partial x} + v_v \frac{\partial T_v}{\partial y} \right) = k_v \frac{\partial^2 T_v}{\partial y^2} \tag{4}$$

LIQUID ($y > \delta_v$)

$$\frac{\partial u_l}{\partial x} + \frac{\partial v_l}{\partial y} = 0 \tag{5}$$

$$\rho_l \left(u_l \frac{\partial u_l}{\partial x} + v_l \frac{\partial u_l}{\partial y} \right) = - \frac{dp_l}{dx} + \mu_l \frac{\partial^2 u_l}{\partial y^2} \tag{6}$$

$$\frac{\partial p_l}{\partial y} = 0 \tag{7}$$

$$\rho_l C_{pl} \left(u_l \frac{\partial T_l}{\partial x} + v_l \frac{\partial T_l}{\partial y} \right) = k_l \frac{\partial^2 T_l}{\partial y^2} \tag{8}$$

LIQUID-VAPOR INTERFACE ($y = \delta_v$)

$$u_v = u_l \tag{9}$$

$$\rho_v \left(u_v \frac{d\delta_v}{dx} - v_v \right) = \rho_l \left(u_l \frac{d\delta_v}{dx} - v_l \right) = \dot{m} \tag{10}$$

$$\mu_v \frac{\partial u_v}{\partial y} = \mu_l \frac{\partial u_l}{\partial y} \tag{11}$$

$$p_v = p_l \tag{12}$$

$$T_v = T_L = T_{sat} \tag{13}$$

$$- k_v \frac{\partial T_v}{\partial y} = - k_L \frac{\partial T_l}{\partial y} + \dot{m} h_{fg} \tag{14}$$

BOUNDARY CONDITIONS ($y = 0, y \to \infty$)

$$\text{At } y = 0;\ u_v = v_v = 0,\ T_v = T_w \tag{15}$$

$$\text{As } y \to \infty;\ u_l \to U_e(x) = C x^m,\ T_l \to T_\infty, \text{ where C is a constant} \tag{16}$$

In this analysis, the constant C is defined as U_0/L_c^m where U_0 is a suitable reference velocity (say $U_0 = U_e$@ $x = L_c$) and L_c is the characteristic length of the wedge. The liquid pressure gradient term in Eq. (6) is determined on the basis of inviscid liquid flow considerations using the external velocity distribution specified in Eq. (16). By using the continuity of pressure requirement [Eq. (12)] and the liquid pressure gradient, the pressure gradient term in the vapor flow [Eq. (2)] is determined as

$$- \frac{dp_l}{dx} = - \frac{dp_v}{dx} = \rho_l U_e \frac{dU_e}{dx}$$

For the vapor film and the liquid boundary layers, following Sparrow et al.[13] and Sparrow and Yu,[14] the following variables are introduced to analyze this nonsimilar two-phase boundary layer flow. (The nonsimilarity is a direct result of the consideration of the buoyancy force acting on the vapor film.)

$$\lambda = \frac{2 \xi U_0 L_c g_x (\rho_l - \rho_v)}{\rho_v U_e^3}, \text{ where } \xi = \frac{(x / L_c)^{m+1}}{m + 1} \tag{17}$$

$$\eta_v = y \left(\frac{m + 1}{2} \frac{U_e}{\nu_v x} \right)^{1/2}, \eta_L = y \left(\frac{m + 1}{2} \frac{U_e}{\nu_L x} \right)^{1/2} \tag{18}$$

$$g(\lambda, \eta_v) = \frac{\psi_v}{\left(\frac{2}{m + 1} \nu_v x U_e \right)^{1/2}}, f(\lambda, \eta_l) = \frac{\psi_l}{\left(\frac{2}{m + 1} \nu_l x U_e \right)^{1/2}} \tag{19}$$

$$\theta_v = \frac{T_v - T_{sat}}{T_w - T_{sat}}, \theta_L = \frac{T_L - T_{sat}}{T_{sat} - T_\infty} \tag{20}$$

As defined by Eq. (17), λ can be interpreted as a nondimensional stream-wise coordinate. An alternative physical interpretation of λ is that it is the buoyancy force parameter, dependent on the Froude number as follows.

$$\lambda = \frac{2 \xi}{Fr} \left(\frac{\rho_l}{\rho_v} - 1 \right) \text{ where } Fr = \frac{U_e^3}{U_0 L_c g_x} \tag{21}$$

η_v and η_l (Eq. 18) are the nondimensional transverse coordinates. (These become similarity coordinates if similarity conditions are exactly satisfied, as is the case for a horizontal flat plate[2] or a wedge flow without considering the buoyancy effects.)[8] The nondimensional stream function and the temperature of the vapor (g, θ_v) and the liquid flow (f, θ_l) are defined by Eq. (19) and Eq. (20), respectively. It is to be noted that under limiting conditions, the above nondimensional variables reduce to the same nondimensional variables defined by others.[2,8]

Using the above nondimensional variables, Eqs. (1)–(16) are transformed into Eqs. (22)–(32) as follows.

VAPOR ($\eta_v < \eta_{v\delta}$)

$$g''' + g\,g'' + \beta\left(\frac{\rho_L}{\rho_v} - g'^2\right) + \lambda = \frac{2(1-2m)}{m+1}\lambda\left(g'\frac{\partial g'}{\partial\lambda} - g''\frac{\partial g}{\partial\lambda}\right) \quad (22)$$

$$\frac{1}{Pr_v}\theta_v'' + g\,\theta_v' = \frac{2(1-2m)}{m+1}\lambda\left(g'\frac{\partial\theta_v'}{\partial\lambda} - \theta_v'\frac{\partial g}{\partial\lambda}\right) \quad (23)$$

LIQUID ($\eta_L > \eta_{L\delta}$)

$$f''' + f\,f'' + \beta\left(1 - f'^2\right) = \frac{2(1-2m)}{m+1}\lambda\left(f'\frac{\partial f'}{\partial\lambda} - f''\frac{\partial f}{\partial\lambda}\right) \quad (24)$$

$$\frac{1}{Pr_L}\theta_L'' + f\,\theta_L' = \frac{2(1-2m)}{m+1}\lambda\left(f'\frac{\partial\theta_L'}{\partial\lambda} - \theta_L'\frac{\partial f}{\partial\lambda}\right) \quad (25)$$

LIQUID-VAPOR INTERFACE ($\eta_v = \eta_{v\delta}$ or $\eta_L = \eta_{L\delta}$)

$$g' = f' \quad (26)$$

$$g + \frac{2(1-2m)}{m+1}\lambda\frac{\partial g}{\partial\lambda} = R^{-1/2}\left(f + 2\lambda\left(\frac{1-2m}{m+1}\right)\frac{\partial f}{\partial\lambda}\right) \quad (27)$$

$$g'' = R^{-1/2} f'' \quad (28)$$

$$\theta_v = 0\,;\ \theta_L = 1 \quad (29)$$

$$Ja_v = \frac{Ja_L\,R^{1/2}\,Pr_v}{Pr_L}\frac{\theta_L'}{\theta_v'}\cdot\frac{Pr_v}{\theta_v'}\left(g + 2\lambda\frac{(1-2m)}{m+1}\frac{\partial g}{\partial\lambda}\right) \quad (30)$$

BOUNDARY CONDITIONS ($\eta_v = 0\,,\ \eta_L \to \infty$)

$$\text{At } \eta_v = 0;\ g' = 0,\ g + 2\left(\frac{1-2m}{m+1}\right)\lambda\frac{\partial g}{\partial\lambda} = 0,\ \theta_v = 1 \quad (31)$$

$$\text{As } \eta_L \to \infty;\ f' \to 1,\ \theta_L \to 1 \quad (32)$$

The above transformed equations are partial differential equations in λ, η coordinate system. Primes refer to differentiation with respect to η_v, η_L as applicable. To solve the above system of equations, the "local similarity" method proposed by Sparrow et al.[13] and Sparrow and Yu[14] is used in the current analysis. Under this approximation, the derivatives with respect to λ are postulated to be small and drop out of the above governing equations [Eqs. (22)–(32)] when λ is large. Physically, a large value of λ means that the stream-wise buoyancy force acting on the vapor film is dominant. As shown in Table 1, the parameter $2\xi/Fr$ [see Eq. (21)] can assume large values (in turn, λ) in most of the flow film boiling situations. The calculations reported in Table 1 were performed for a 90° included angle wedge (horizontal and vertical directions) using the properties of water at atmospheric pressure. The characteristic length of the wedge varied from 1 cm to 15 cm, and $U_{e@x=L_c}$ is assumed equal to U_∞.

With the "local similarity" approximation, Eqs. (22)–(32) reduce to the following form.

VAPOR ($\eta_v < \eta_{v\delta}$)

$$g''' + g\,g'' + \beta\left(\frac{\rho_L}{\rho_v} - g'^2\right) + \frac{2\xi}{Fr}\left(\frac{\rho_L}{\rho_v} - 1\right) = 0 \quad (33)$$

$$\theta_v'' + Pr_v\,g\,\theta_v' = 0 \quad (34)$$

LIQUID ($\eta_L > \eta_{L\delta}$)

$$f''' + f\,f'' + \beta\left(1 - f'^2\right) = 0 \quad (35)$$

$$\theta_L'' + Pr_L\,f\,\theta_L' = 0 \quad (36)$$

LIQUID-VAPOR INTERFACE ($\eta_v = \eta_{v\delta}$ or $\eta_L = \eta_{L\delta}$)

$$g' = f' \quad (37)$$

$$g = R^{-1/2} f \quad (38)$$

$$g'' = R^{-1/2} f'' \quad (39)$$

$$\theta_v = 0\,;\ \theta_L = 1 \quad (40)$$

$$Ja_v = \frac{Ja_L\,R^{-1/2}\,Pr_v}{Pr_L}\frac{\theta_L'}{\theta_v'}\cdot\frac{Pr_v}{\theta_v'}\,g \quad (41)$$

BOUNDARY CONDITIONS ($\eta_v = 0\,,\ \eta_L \to \infty$)

$$\text{At } \eta_v = 0;\ g' = 0,\ g = 0,\ \theta_v = 1 \quad (42)$$

$$\text{As } \eta_L \to \infty;\ f' \to 1,\ \theta_L \to 1 \quad (43)$$

These equations [Eqs. (33)–(43)] are solved (described later) for velocity and temperature profiles, and the results are displayed via skin friction coefficient and Nusselt number, namely,

$$C_{f_x} = \frac{\mu_v\left\langle\frac{\partial u_v}{\partial y}\right\rangle_{y=0}}{\frac{1}{2}\rho_L U_\infty^2} \Rightarrow \frac{C_{f_x}\sqrt{Re_x}}{2} = R^{1/2}\left(\frac{m+1}{2}\right)^{1/2} g''(0) \quad (44)$$

$$Nu_x = \frac{h\,x}{k_v} = \frac{\left\langle\frac{\partial T_v}{\partial x}\right\rangle x}{(T_w - T_{sat})} \Rightarrow \frac{Nu_x}{\sqrt{Re_x}}\left(\frac{\mu_v}{\mu_L}\right) = -R^{1/2}\left(\frac{m+1}{2}\right)^{1/2}\theta_v'(0) \quad (45)$$

Solution Methodology

Of the eight explicitly prescribable parameters in the governing equations [Eqs. (33)–(45)] seven are $\frac{2\xi}{Fr}$ (buoyancy force

TABLE 1

MAGNITUDE OF THE PARAMETER $\frac{2\xi}{Fr}$

90° wedge, 1 cm ≤ L_c ≤ 15 cm, Vertical and Horizontal Orientations			
Re_{L_c}	T_∞ = 20°C	T_∞ = 60°C	T_∞ = 100°C
10	$2.34 \times 10^5 - 1.7 \times 10^9$	$3.6 \times 10^5 - 2.6 \times 10^9$	$5.5 \times 10^5 - 4.0 \times 10^9$
10^2	$2.34 \times 10^3 - 1.7 \times 10^7$	$3.6 \times 10^3 - 2.6 \times 10^7$	$5.5 \times 10^3 - 4.0 \times 10^7$
10^3	$2.3 \times 10 - 1.7 \times 10^5$	$3.6 \times 10 - 2.6 \times 10^5$	$5.5 \times 10 - 4.0 \times 10^5$
10^4	$2.3 \times 10^{-1} - 1.7 \times 10^3$	$3.6 \times 10^{-1} - 2.6 \times 10^3$	$5.5 \times 10^{-1} - 4.0 \times 10^3$
5×10^5	$9 \times 10^{-5} - 0.68$	$1.4 \times 10^{-4} - 1.05$	$2.2 \times 10^{-4} - 1.05$

parameter), $\beta = \frac{2m}{m+1}$ (pressure gradient parameter), $\frac{\rho_L}{\rho_v}$ (density ratio parameter), $R = \frac{\rho_v \mu_v}{\rho_L \mu_L}$ (density-viscosity product ratio parameter), Pr_v (vapor Prandtl number), Pr_L (liquid Prandtl number) and Ja_L (liquid subcooling parameter, namely, liquid Jakob number). For the choice of the eighth parameter, it is to be noted that $\eta_{v\delta}$ (nondimensional vapor film thickness) and Ja_v (wall superheat parameter, namely, vapor Jakob number) are related implicitly to each other by Eq. (41). One of these would suffice to obtain a solution to the above governing equations. As done earlier,[8,15] the nondimensional vapor film thickness $\eta_{v\delta}$ is chosen to be the eighth parameter, and the corresponding wall superheat parameter Ja_v is calculated from Eq. (41) as a final step in the solution of the governing equations [Eqs. (33)–(45)]. Such a procedure reduces the number of iterations needed to obtain a solution as discussed in our earlier study.[8]

A fourth-order Runge-Kutta method with a shooting technique [to find the missing wall shear, $g''(0)$] is used to solve the momentum equations of the vapor and liquid flow [Eqs. (33) and (35) along with the conditions Eqs. (37)–(39), (42) and (43)] for the vapor and liquid velocity profiles. This approach is basically an extension of the solution strategy used for single-phase boundary layer equations,[16] and its application to two-phase boundary layer film boiling flow is described in detail in our earlier paper.[8] Using these velocity profiles, the energy equations [Eqs. (34) and (36) along with the conditions Eqs. (40) and (42)–(43)] of the vapor and liquid phases are solved in an implicit finite-difference form. The first- and second-order cross-stream derivatives in the energy equations were replaced by central difference approximations, which resulted in a tri-diagonal matrix for each phase. These matrices were solved by a simple Gaussian elimination scheme to yield the temperature profiles.

Using the temperature profiles, the temperature gradient of vapor at the wall, $\theta_v'(0)$ and the temperature of the liquid at the liquid-vapor interface $\theta_L'(\eta_{v\delta})$ was determined by a second-order, forward finite-difference approximation. The temperature gradient of the vapor at the liquid-vapor interface, $\theta_v'(\eta_{v\delta})$ is calculated by a second-order backward difference approximation. The velocity and temperature profiles in combination with the gradients then are used to evaluate nondimensional skin friction, heat-transfer and wall superheat parameters from Eqs. (44), (45), and (41), respectively. The flow chart of the computer program is given in Fig. 2.

During this analysis, the effect of approximating infinity in the liquid boundary layer by a finite distance, the tolerance limit on satisfying the boundary conditions at the outer edge of the liquid boundary layer, and the grid spacing in the vapor film and the liquid layer were examined for various conditions. These tests and random checking of the results during the course of computations were used to assess the numerical uncertainty of the results. Accuracy was satisfied up to the third decimal place in most of these calculations. Based on these tests, the free-stream boundary conditions at infinity were satisfied at a finite dimension, $\eta_{L,max} = 6$, with an accuracy of $\varepsilon = 10^{-4}$. The combination of grid sizes used in this study, as used earlier,[8] is given in Table 2.

TABLE 2

GRID SIZES

η_v	$\Delta\eta_v$
0.001 - 0.005	0.0001
0.005 - 0.5	0.001
0.5 - 1.0	0.005
1.0 - 5.0	0.01
$\Delta\eta_L$	= 0.03

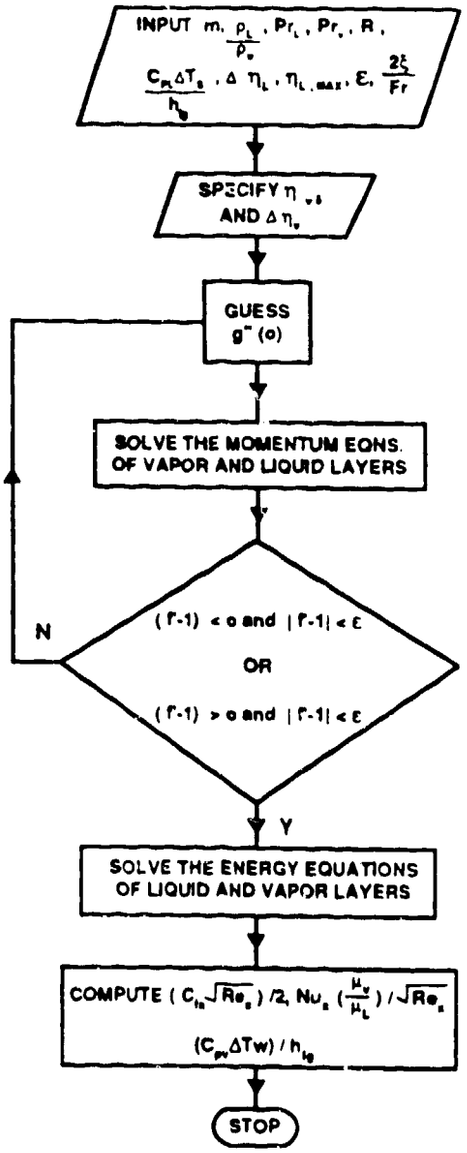

Fig. 2. Flow Chart.

Because of the coupled nonlinearity of the governing differential equations, the fourth-order Runge-Kutta method along with the shooting technique used in the solution methodology are sensitive to the starting input value of $g''(0)$. Typically, the initial input value of $g''(0)$ at prescribed values of $\eta_{v\delta}$ and other parameters is chosen by following the previous patterns of changes of $g''(0)$ with $\eta_{v\delta}$. Choosing a low value of $\eta_{v\delta}$ initially and increasing it steadily would facilitate easier guessing of the starting input value of $g''(0)$. After the initial input value of $g''(0)$ is given to start the Runge-Kutta procedure, convergence is obtained by using a bisection method to refine the wall shear $g''(0)$. If the flow is accelerated strongly (i.e., at large parametric values of the buoyancy force parameter $\frac{2\xi}{Fr}$, say 100), the tolerance limit of satisfying the free-stream boundary condition was increased from 10^{-4} to 10^{-3} or 10^{-2}.

Referring to the flow chart (Fig. 2), it is to be noted that two convergence criteria are specified for the solution of vapor and liquid momentum equations. The first one, $(f' - 1) < 0$ and $|f' - 1| < \varepsilon$, is used when the vapor is flowing faster than the liquid and the second criterion, $(f' - 1) > 0$ and $|f' - 1| < \varepsilon$, is used when the liquid is

flowing faster than the vapor. When the liquid-vapor interface is nearly equal to the free stream velocity, the liquid boundary layer does not exist, and computations with either condition produced essentially the same results.

Discussion of Results

The current numerical procedure initially was verified by reproducing the results of Ito and Nishikawa[15] and Nakayama,[7] which are the limit cases for the current analysis. Comparisons with Nakayama's results are reported in our earlier study[8] and for the sake of brevity, they are not repeated. A water-steam system at atmospheric pressure with subcoolings from 20 to 100°C and encompassing wall superheats of 100 to 600°C is considered in this study. Fluid properties were evaluated at the respective film temperatures of the vapor and liquid. Because the vapor Prandtl number (= 1) varies negligibly in the above wall superheat range, a constant value of unity was assigned. With the computed parameters, calculations were performed by varying one parameter at a time. Calculations typically were performed at the limiting values of each parameter.

It is to be noted that on a vertical wedge with an upward flow (Fig. 1), the stream-wise component of buoyancy force acting on the vapor film always aids the vapor flow on both surfaces of the wedge. However, on a horizontal wedge (Fig. 1), it is favorable to the flow on the upper surface and opposes the flow on the lower surface. Thus, the current analysis with a favorable stream-wise component of buoyancy force is equally valid for the vertical wedge with an upward flow and the upper surface of a horizontal wedge.

Figures 3–5 show the influence of the favorable local buoyancy force parameter, $\frac{2\xi}{Fr}$, on local skin friction and heat transfer. A low value of the buoyancy force parameter, $\frac{2\xi}{Fr}$, implies that either the nondimensional stream-wise length ξ is small or the local

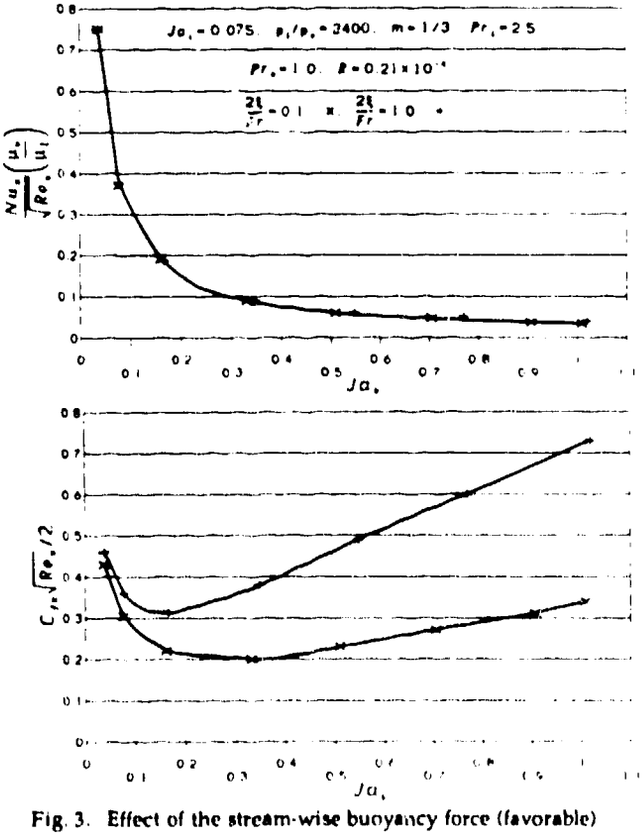

Fig. 3. Effect of the stream-wise buoyancy force (favorable) parameter, $2\xi/Fr$.

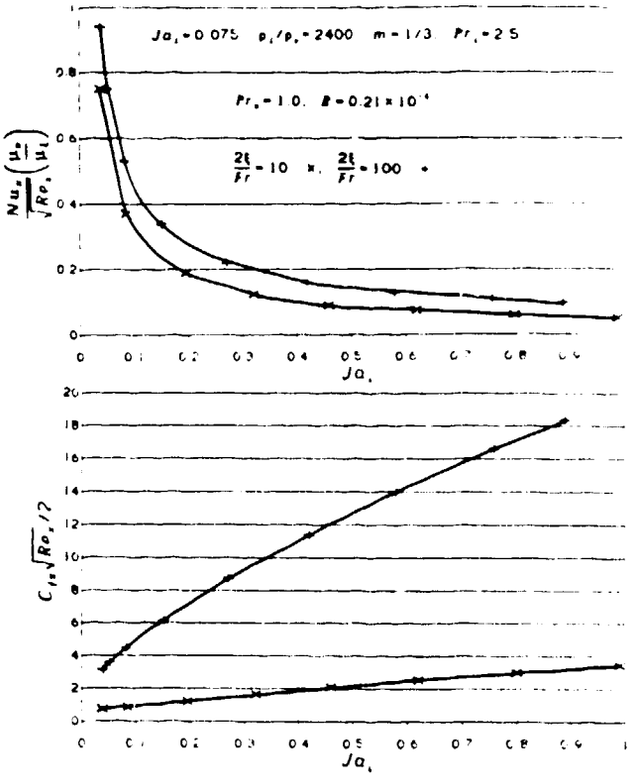

Fig. 4. Effect of the stream-wise buoyancy force (favorable) parameter, $2\xi/Fr$.

Froude number is large (meaning domination of velocity effects over gravity effects). As $\frac{2\xi}{Fr}$ increases from 0.1 and 100 (which implies a domination of the favorable buoyancy force driving the vapor flow), Figs. 3 and 4 illustrate that the local skin friction parameter, $C_{fx}\sqrt{Re_x}/2$, and the local heat-transfer parameter, $\frac{Nu_x}{\sqrt{Re_x}}\left(\frac{\mu_v}{\mu_l}\right)$, also increase. This trend is understandable because favorable buoyancy force accelerates the vapor film flow, resulting in higher vapor flow velocities (Fig. 5), which should cause an increase in local wall skin friction and heat transfer.

At low values of the buoyancy force parameter, $\frac{2\xi}{Fr} = 0.1, 1$, the skin friction parameter, $C_{fx}\sqrt{Re_x}/2$, initially decreases, reaches a minimum, and starts increasing with increasing wall superheat parameter Ja_v. This type of "turn-around" behavior of the local skin friction parameter with increased heating of the wedge is the result of the domination of the streamwise pressure gradient and the buoyancy force driving the vapor film (as to be demonstrated later) at higher wall superheats. Additionally, it can be observed that the local skin friction parameter, $C_{fx}\sqrt{Re_x}/2$, at higher values of the buoyancy force parameter, $\frac{2\xi}{Fr} = 10, 100$, does not exhibit the bucket-type phenomenon with increased heating of the wedge; rather, the trend is a monotonic increase with an increase in the wall superheat parameter, Ja_v. Although the "bucket" type of phenomenon exhibited by the skin friction parameter has been observed earlier by Nakayama[7] (whose analysis does not consider the effects of stream-wise buoyancy force on the vapor flow), the latter trends exhibited by the local skin friction parameter at higher values of the buoyancy force parameter cannot be realized without considering the buoyancy effects.

The above trends exhibited by the skin friction parameter can be explained in a simple manner (on a first-order basis) by approximating the vapor film flow locally as a "Couette flow." Such a

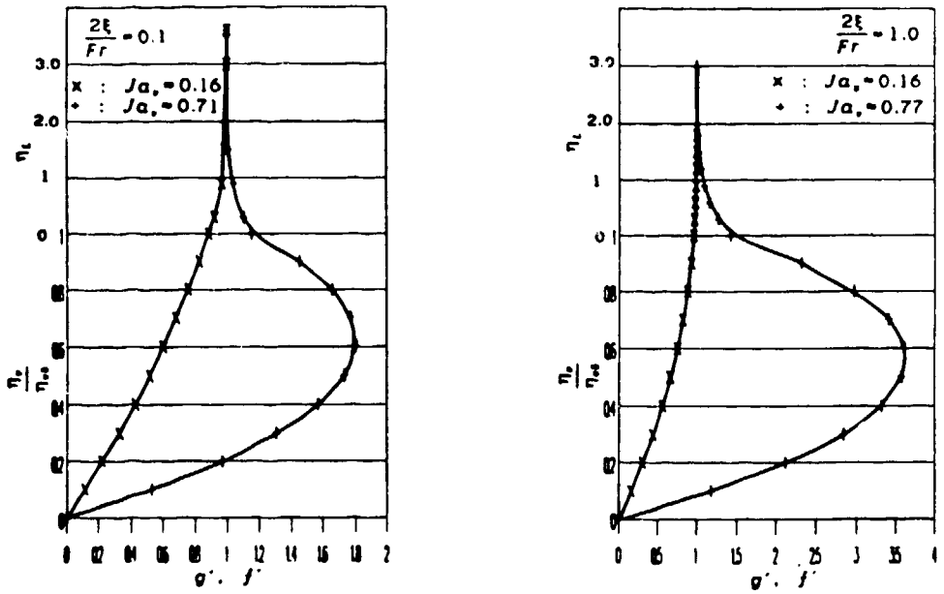

Fig. 5. Velocity profiles showing the effects of stream-wise buoyancy for parameter, $2\xi/Fr$.

model has been used by these authors to explain some of the trends in forced convection film boiling on a wedge (without buoyancy effects).[8] An integration of the Couette flow equations of the vapor flow leads to a quadratic velocity profile, and using this, the wall shear on the wedge can be written as

$$\tau_w = \mu_v \left\langle \frac{\partial u_v}{\partial y} \right\rangle_{y=0} \equiv \mu_v \frac{u_v}{\delta_v} + \frac{\delta_v}{2} \left\{ \rho_L U_e \frac{dU_e}{dx} + (\rho_L - \rho_v) g_x \right\} \qquad (46)$$

In the nondimensional variables of the current analysis, the above equation is rewritten as

$$g''(0) \equiv \frac{g_x}{\eta_{v\delta}} + \frac{\eta_{v\delta}}{2} \frac{2m}{m+1} \frac{\rho_L}{\rho_v} + \frac{\eta_{v\delta}}{2} \frac{2\xi}{Fr} \left(\frac{\rho_L}{\rho_v} - 1 \right) \qquad (47)$$

In the above equation, $g''(0)$ comprises the viscous shear contribution (without the effect of pressure gradient, for example, a flat-plate film boiling flow) of the vapor film [first term on the right side of Eq. (47)], the influence of the external stream-wise pressure gradient on the flow (second term), and the effect of the local stream-wise component of buoyancy on the vapor film (third term). When the buoyancy force driving the vapor film is low, the skin friction characteristics are dominated by the first term at low wall superheats and by the second term at higher wall superheats. Predictions in Table 3 (calculated by using numerically obtained values of $g_x, \eta_{v\delta}$) at low values of $\frac{2\xi}{Fr}$ (say , 0.1) illustrate this hypothesis very clearly. Thus, the turn-around behavior of the local skin friction parameter with increased heating of the wedge (i.e., increasing Ja_v) is a result of the domination of the stream-wise pressure gradient and the buoyancy force driving the flow at higher wall superheats. At a higher value of $\frac{2\xi}{Fr}$ (say 100), predictions in Table 3 show that the skin friction behavior is dominated by the buoyancy force term in Eq. (47). Thus, the increasing trend of the local skin friction parameter with increased heating of the wedge (as observed in Fig. 4) can be attributed to the overwhelming domination of the streamwise buoyancy force. Figures 3 and 4 also show that the increase in the buoyancy force parameter causes the local wall heat-transfer parameter, $\frac{Nu_x}{\sqrt{Re_x}} \left(\frac{\mu_v}{\mu_l} \right)$, to increase; however, the increase is not as large as the skin friction parameter.

The influence of the pressure gradient parameter, β, on the local skin friction and heat transfer is shown in Fig. 6. Figure 6 shows that higher values of the pressure gradient parameter, β, improves the local wall heat transfer and wall skin friction. An examination of Eqs. (33) and (47) reveals that the pressure gradient parameter, β, and the density ratio parameter, ρ_L/ρ_v, should qualitatively exert the same influence as the favorable buoyancy force parameter, $\frac{2\xi}{Fr}$, because an increase in these parametric values signifies the acceleration of the film boiling flow leading to increased wall skin

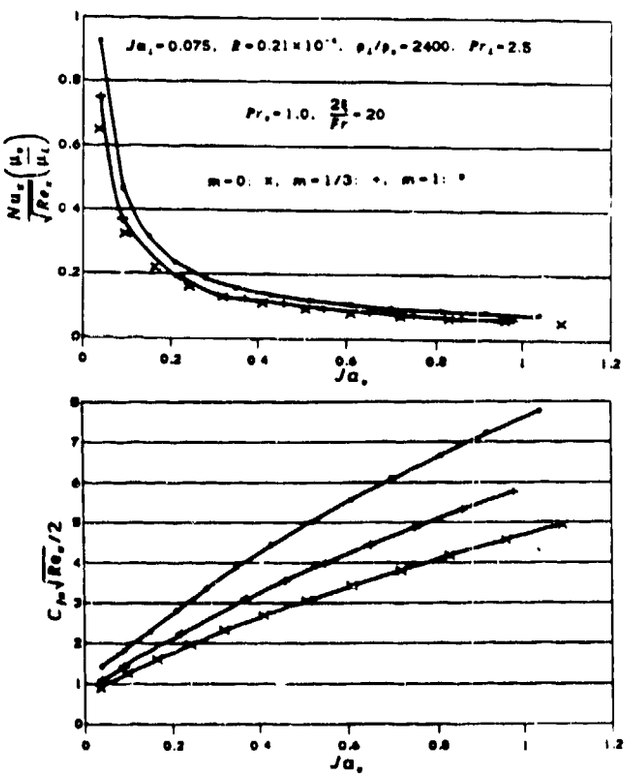

Fig. 6. Influence of the pressure gradient parameter, m.

TABLE 3

CALCULATIONS ILLUSTRATING COUETTE FLOW HYPOTHESIS

Ja_v	$g''(0)$	$\eta_{v\delta}$	g'_i	$\frac{g'_i}{\eta_{v\delta}}$	$\frac{\eta_{v\delta}}{2}\frac{2m}{m+1}\frac{\rho_D}{\rho_v}$	$\frac{\eta_{v\delta}}{2}\frac{2}{Fr}\left[\frac{\rho_L}{\rho_v}-1\right]$
$\frac{2\xi}{Fr_L} = 0.1$						
0.159	58.8	0.02	0.888	44.4	12	2.4
0.333	54.05	0.04	1.01	25.25	24	4.8
0.705	72	0.08	1.152	14.4	48	9.6
$\frac{2\xi}{Fr_L} = 10.0$						
0.195	330.4	0.02	1.57	78.50	12	239.9
0.322	433.23	0.03	1.96	65.33	18	359.9
0.62	803.87	0.06	2.89	48.17	36	719.7

friction and heat transfer. To conserve space, figures illustrating the effect of the density ratio parameter ρ_L/ρ_v on local skin friction and wall heat transfer are not shown. The density ratio parameter, ρ_L/ρ_v, varies from approximately 2000 to 2800 in the current analysis. Although the wall heat-transfer parameter, $\frac{Nu_x}{\sqrt{Re_x}}\left(\frac{\mu_v}{\mu_L}\right)$, shows an increase as the density ratio parameter increases, this improvement is marginal.

Figure 7 shows the influence of the liquid subcooling parameter, Ja_L. $Ja_L = 0$ represents saturated water, and $Ja_L = 0.15$ represents highly subcooled (say, 20°C) water at atmospheric pressure. With increased liquid subcooling, the local wall heat transfer parameter, $\frac{Nu_x}{\sqrt{Re_x}}\left(\frac{\mu_v}{\mu_L}\right)$, increases (signifying an increase in the local wall heat-transfer coefficient). This is to be expected because $h = k_v/\delta_v$ and subcooling the liquid will decrease the vapor film thickness δ_v. This trend also can be conjectured from the interfacial energy balance [Eq. (14)], which implies that as the liquid subcooling increases, vapor generation at the liquid vapor interface decreases because less energy is available for vapor production. Consequently, an increase in liquid subcooling results in less vapor generation, leading to thinner vapor films. As shown in Fig. 7, subcooling the liquid (at the parametric values shown in the figure) decreases the wall skin friction parameter. This trend is to be anticipated on the basis of Eq. (47) derived from the Couette flow hypothesis. For this buoyancy-dominated flow, $\left(\frac{2\xi}{Fr} = 20\right)$, similar to the trends as shown earlier for $\frac{2\xi}{Fr} = 100$ in Table 3, the buoyancy force term in Eq. (47) dominates the characteristics of the wall skin friction, and the influence of the other two terms in Eq. (47) is minor. The contribution of the buoyancy force term in Eq. (47) is linearly proportional to the vapor film thickness. Any decrease in vapor film thickness as a result of increased liquid subcooling will reduce the local wall skin friction as shown in Fig. 7.

The influence of the density-viscosity ratio parameter R and the liquid Prandtl number Pr_L are not shown in order to conserve space. For the water-steam system under consideration, the density-viscosity ratio parameter R varies from 0.155×10^{-4} to 0.272×10^{-4} and the liquid Prandtl number varies from 1.75 to 3.0. The density-viscosity ratio parameter affects the local wall heat-transfer predictions marginally in the parametric range considered. An increase in the liquid Prandtl number translates the skin friction and heat-transfer curves toward lower wall superheats.

As mentioned earlier, on the bottom surface of the horizontal wedge, the stream-wise component of buoyancy force acting on the vapor film is adverse (Fig. 1), i.e., it opposes the motion of vapor film. In the current analysis, this effect is simulated by the negative values given to the buoyancy force parameter $\frac{2\xi}{Fr}$. Figures 8 and 9 show the influence of opposing buoyancy force on flow film

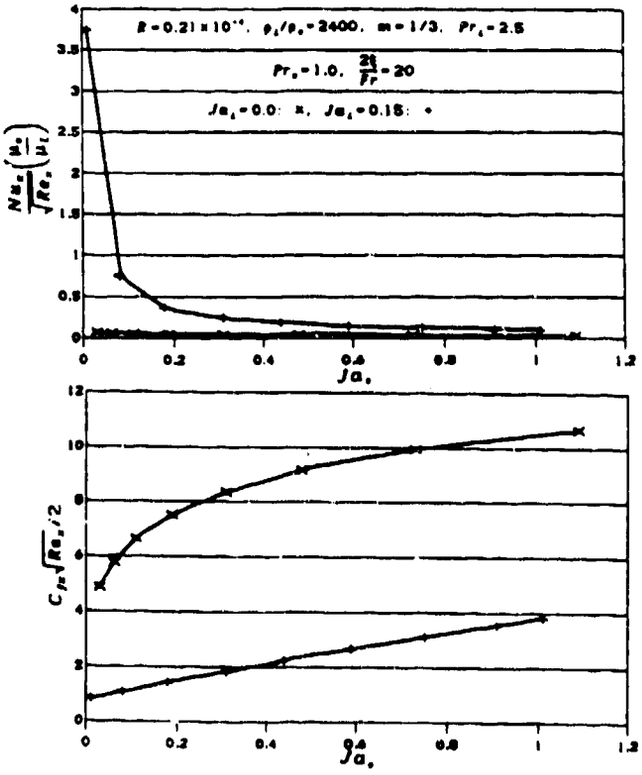

Fig. 7. Influence of liquid subcooling parameter, Ja_L.

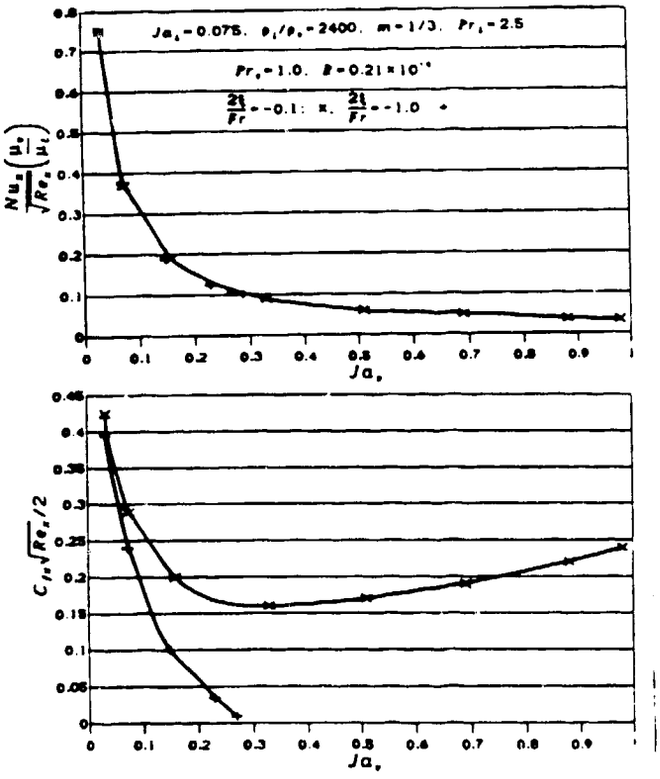

Fig. 8. Opposing stream-wise buoyancy force parameter effect, $2\xi/Fr$

boiling. This opposing buoyancy force slows down the vapor film, and the skin friction at the wall reduces. If the opposing buoyancy force is large enough (as signified by the larger value taken by $\frac{2\xi}{Fr}$, -1.0), the vapor film may stagnate and separate. A typical velocity profile of the vapor film close to separation is illustrated in the right panel of Fig. 9. Once again, the effect of the opposing buoyancy force parameter is marginal in wall heat-transfer predictions (Fig. 8).

Concluding Remarks

Laminar forced convection film boiling flow on a wedge is analyzed. Because of its finite thickness, the wedge will impose a stream-wise pressure gradient on the flow, which is the case for the flow over any finitely thick body. For a water-steam system at atmospheric pressure considered in this study, the density difference between the liquid and vapor is large enough to warrant consideration of the buoyancy force on the film boiling flow. A two-phase boundary layer model considering the above two effects for the first time is proposed, and a numerical solution to the governing equations is obtained by using the concept of local similarity. Below are our major observations.

1. Unlike the horizontal flat plate geometry, the skin friction on a wedge in a film boiling flow may increase beyond the single-phase (all liquid) flow level. This feature is attributed to the domination of the stream-wise buoyancy force and the external pressure gradient driving the vapor flow.
2. A turn-around behavior of the wall skin friction parameter with increased heating of the wedge (as demonstrated by earlier studies)[6,8] is possible only when the buoyancy force driving the vapor film is "low."
3. On the lower surface of a horizontally aligned wedge in a film boiling flow, the buoyancy force on vapor film acts adversely to the flow direction. Under such conditions the current study demonstrates vapor flow separation; a feature unnoticed until now.
4. Wall heat-transfer predictions, as opposed to skin friction predictions, demonstrate a secondary dependence on the buoyancy force parameter.
5. Subcooling of liquid increases the wall heat transfer coefficient and translates the local skin friction curves toward higher wall superheats.

References

1. Bradfield, W. S., Barkdoll, R. O., and Bryne, J. T., "Some Effects of Boiling on Hydrodynamic Drag," *International Journal of Heat and Mass Transfer*, Vol. 5, 1962, pp. 615-622.
2. Cess, R. D., and Sparrow, E. M., "Film Boiling in Forced Convection Boundary-Layer Flow," *ASME Journal of Heat Transfer*, Vol. 84, 1961, pp. 370-376.

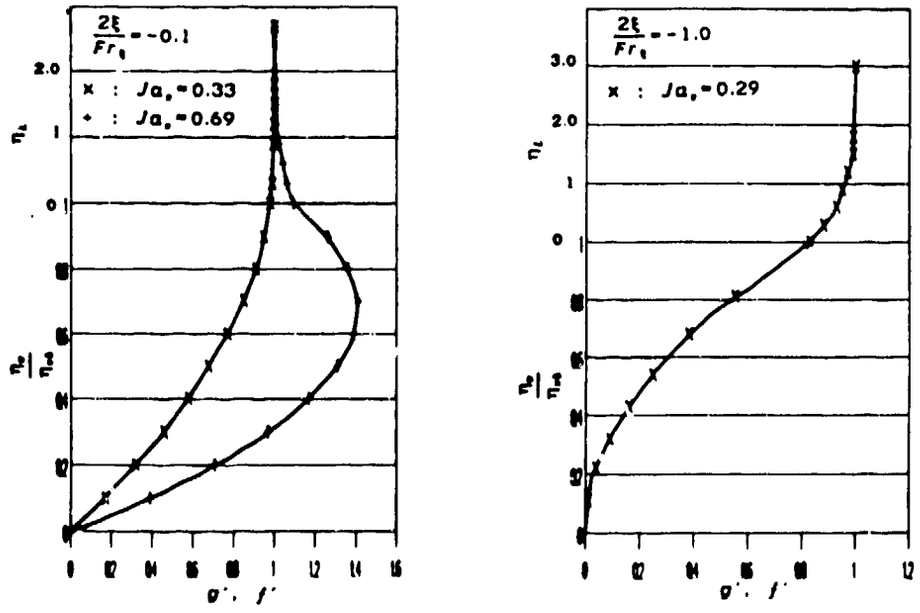

Fig. 9. Velocity profiles as influenced by the adverse buoyancy force parameter $2\xi/Fr$.

3. Chappidi, P. R., "Drag Characteristics of Objects in Two-Phase Boiling Flows," Ph.D. Thesis, University of Central Florida, Orlando, August 1989.

4. Cho, D. H. and Lambert, G. A. "Effect of Boiling on Particle Drag," *Nuclear Engineering and Design*, Vol. 108, 1988, pp 523-524.

5. Gay, A., "Film Boiling Heat Transfer and Drag Reduction," Convair Aerospace Division Report, GDCA-DDB-71-001, San Diego, California, 1971.

6. Walsh, S. K., and Wilson, S. D. R., "Boundary-Layer Flow in Forced-Convection Film Boiling on a Wedge," *International Journal of Heat and Mass Transfer*, Vol. 22, 1979, pp. 569-576.

7. Nakayama, A., "Subcooled Forced Convection Film Boiling in the Presence of a Pressure Gradient," *Journal of AIAA*, Vol.24, 1986, pp. 230-236.

8. Chappidi, P. R., and Gunnerson, F. S., "A Numerical Study of the Skin Friction and Heat Transfer Characteristics of a Wedge in Film Boiling Flow," *ASME Proceedings of the 1988 National Heat Transfer Conference*, Houston, Texas, Vol. 2., 1988, 475-486.

9. Hsu, Y. Y., and Westwater, J. W., "Approximate Theory for Film Boiling on Vertical Surfaces," *Chemical Engineering Progress Symposium Series*, Vol. 56, No. 30, 1960, pp. 15-24.

10. Bromley, L. A., Leroy, N. R. and Robbers, J. A., "Heat Transfer in Forced Convection Film Boiling," *Industrial and Engineering Chemistry*, Vol. 45, 1953, pp. 2639-2646.

11. Stevens, J. W. and Witte, L. C., "Destabilization of Vapor Film Flow Around Spheres," *International Journal of Heat and Mass Transfer*, Vol. 16, 1973, pp. 669-678.

12. Chappidi, P. R., Pasamehmetoglu, K. O., and Gunnerson, F. S., "The Influence of Surface Radiation on Forced Convection Film Boiling," to be presented at *International Symposium on Gas-Liquid Two-Phase Flows, ASME Winter Annual Meeting*, Dallas, Texas, November 25-30, 1990.

13. Sparrow, E. M., Quack, H., and Boerner, C. J., "Local Nonsimilarity Boundary-Layer Solutions," *Journal of AIAA*, Vol. 8, 1970, pp. 408-414.

14. Sparrow, E. S., and Yu. H. S., "Local Non-Similarity Thermal Boundary-Layer Solutions," *ASME Journal of Heat Transfer*, 1971, Vol. 92, pp. 328-334.

15. Ito, T., and Nishikawa, K., "Two-Phase Boundary-Layer Treatment of Forced-Convection Film Boiling," *International Journal of Heat and Mass Transfer*, Vol. 9, 1966, pp. 117-130.

16. Chow, C. Y., *An Introduction to Computational Fluid Mechanics*, corrected edition (Seminole Publishing Company, Colarado, 1983).